



OPEN ACCESS

EDITED BY
Jialai Wang,
University of Alabama, United States

REVIEWED BY
Peiyuan Chen,
Anhui University of Science and
Technology, China
Fengjuan Liu,
Mapei Corp, United States

*CORRESPONDENCE
Shunkai Li,
lishunkai7910@163.com
Ping Chen,
chenping8383@188.com

SPECIALTY SECTION
This article was submitted to Structural
Materials,
a section of the journal
Frontiers in Materials

RECEIVED 31 August 2022
ACCEPTED 24 November 2022
PUBLISHED 05 December 2022

CITATION
Zhang Z, Li S, Chen P, Liu X and Wang J
(2022), Mitigating shrinkage in ultra-
high performance concrete using MgO
expansion agents with different
activity levels.
Front. Mater. 9:1033467.
doi: 10.3389/fmats.2022.1033467

COPYRIGHT
© 2022 Zhang, Li, Chen, Liu and Wang.
This is an open-access article
distributed under the terms of the
[Creative Commons Attribution License
\(CC BY\)](https://creativecommons.org/licenses/by/4.0/). The use, distribution or
reproduction in other forums is
permitted, provided the original
author(s) and the copyright owner(s) are
credited and that the original
publication in this journal is cited, in
accordance with accepted academic
practice. No use, distribution or
reproduction is permitted which does
not comply with these terms.

Mitigating shrinkage in ultra-high performance concrete using MgO expansion agents with different activity levels

Zhanqiang Zhang¹, Shunkai Li^{2,3,4*}, Ping Chen^{2,3,4*}, Xiaoyan Liu²
and Jingyang Wang¹

¹College of Materials Science and Engineering, Guilin University of Technology, Guilin, China, ²College of Civil Engineering and Architectural, Guilin University of Technology, Guilin, China, ³Guangxi Key Laboratory of New Energy and Building Energy Saving, Guilin, China, ⁴Collaborative Innovation Center for Exploration of Nonferrous Metal Deposits and Efficient Utilization of Resources in Guangxi, Guilin, China

To mitigate the shrinkage properties of ultra-high performance concrete (UHPC), MgO expansion agents (MEAs) with different activity levels (R-MEA, M-MEA, and S-MEA) were prepared and incorporated into UHPC. The effect of MEA activity on the mechanical properties and volumetric stability of UHPC were evaluated by using hydration heat tests, XRD-Rietveld quantitative analysis, MIP, X-CT and SEM. The results showed that MEA addition reduces the mechanical properties of UHPC, especially at high activity levels. However, it is beneficial for compensating early shrinkage. By combining MIP and X-CT analyses, it was found that MEA effectively increases the porosity of UHPC, with R-MEA (with the strongest activity) increasing it most. The w/b ratio had a greater effect on MEA hydration than the activity level. At lower w/b ratios, R-MEA reduced autogenous shrinkage even less effectively than M-MEA. Considering both the mechanical properties and shrinkage-reducing effect, it is recommended to prepare shrinkage-reducing UHPC with a w/b ratio of 0.18 and moderately reactive M-MEA.

KEYWORDS

MgO expansion agents, activity, w/b ratio, autogenous shrinkage, ultra-high-performance concrete

1 Introduction

Ultra-high performance concrete (UHPC) is a new type of cementitious composite (Richard and Cheyrezy, 1995), which the engineering community has called the most innovative cementitious engineering material of recent years. As UHPC requires a meager water-binder ratio (w/b ratio), high fineness admixture addition, substantial cement dosage, and no coarse aggregate when mixing (Yoo et al., 2013; Li J. et al., 2020). The early stage is usually accompanied by significant shrinkage, which may trigger structural cracking and reduce structural performance and service life. In some studies conducted in China and Japan, the amount of shrinkage reached a staggering 61.3–86.5% (Chen, 2018).

It implies that the early shrinkage of UHPC is mainly determined by its autogenous shrinkage, therefore, in order to reduce the risk of specimens cracking, it is crucial to reduce the autogenous shrinkage.

The main methods reported to reduce autogenous shrinkage are the addition of shrinkage-reducing agents (SRA), expansion agents (EA), or a super absorbent polymer (SAP) to the concrete (Liu et al., 2022). An SRA will delay cement hydration and increase its setting time, which is not conducive to the early strength development of UHPC (Wang et al., 2021). The SAPs are expensive and leave holes in the cement when water is released. Added SAP may absorb additional internal curing water, which increases porosity and may reduce the strength of the concrete (Kong and Zhang, 2013; Kong and Zhang, 2014; Dang et al., 2017). Therefore, the addition of expansion agents is the most direct and effective way to achieve shrinkage reduction in UHPC. Yoo et al. (Yoo et al., 2019) found when 6% and 8% calcium sulfoaluminate (CSA) were added into UHPC, its shrinkage rates decreased by about 7% and 10%, respectively. Shen et al. (Shen et al., 2020) found that a calcium-sulfoaluminate-CaO-based expansive agent (CSA-CaO EA) effectively reduced the autogenous shrinkage of UHPC. However, the use of CSA, CSA-CaO EA and CaO-type expansion agent all involve the following problems (Juenger and Siddique, 2016; Ruan and Unluer, 2016): 1) A poorly adjustable expansion process; 2) a hydration process that requires large amounts of water, which is difficult to achieve in dry engineering environments; and 3) the origin of the expansion is unstable. Therefore, there is an urgent need to develop a new type of expansion agent suitable for UHPC. MgO expansion agent (MEA) is a new type of admixture, and its reaction mechanism in concrete contains the theory of water absorption and expansion by (Mehta, 1973), crystal growth theory by (Chatterji, 1995) and crystallization pressure driven theory by (Deng, 1990). Among them, a representative one is the theory of Deng et al., which suggests that the expansion force of $Mg(OH)_2$ originates from the generation and development of $Mg(OH)_2$ crystals, and the amount of expansion depends on the location, morphology and size of $Mg(OH)_2$ crystals.

Attention was first drawn to MgO in concrete in relation to its detrimental effects on the volume stability of cement materials (Mo et al., 2014). It was not until the dam project in China that it was really realized that it could be used as an expansion agent, and its development history is just over 40 years. As an excellent performance expansion agent, it has the advantage of low activity, a slow hydration rate, and delayed micro-expansion characteristics. It can make concrete produce specific pre-compression stress characteristics during hardening, reduce volume shrinkage and improve crack resistance. At the same time, it can replace part of the cement and, more importantly, less water is consumed in the hydration reaction (Choi et al., 2013; Choi et al., 2014; Yang et al., 2021). Recently, researchers have found that MEA can compensate for the early shrinkage of

UHPC (Li, 2012; Wang et al., 2022), and it has been applied in practical engineering (Li S. et al., 2020). The researchers used different activity levels of MEA and found that the early expansion rate of high-activity MEA is more rapid than that of low-activity, but the expansion stops earlier (Cao et al., 2018; Cao and Yan, 2019). Meanwhile, the late expansion rate of low-activity MEA is faster and the total expansion time is longer. This indicates that the shrinkage-reduction effect of concrete is related to MEA activity level. Unfortunately, the impact of MEA activity level on the performance of UHPC is still poorly understood. In this paper, the effects of MEA with different activity levels on the mechanical properties and early deformation of UHPC were investigated and the expansion mechanism of MEA was explained. Hydration products with different w/b ratios were quantitatively characterized by XRD-Rietveld quantitative analysis, and all pore sizes (connectivity pores and independent pores) were measured using mercury intrusion porosimetry (MIP) and X-ray computed tomography (X-CT). The results provide an effective way to reduce the autogenous shrinkage of UHPC.

2 Materials and methods

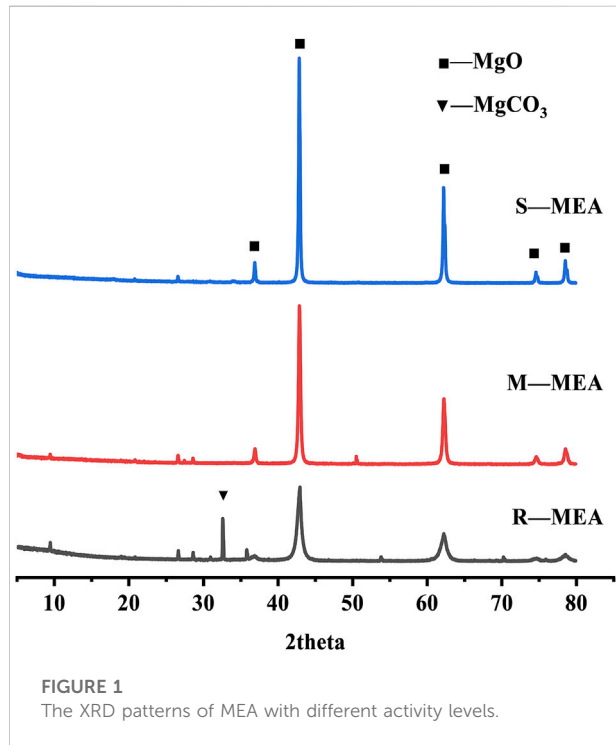
2.1 Experimental materials

Ordinary portland cement (OPC, P.O 42.5) was obtained from Hailuo Cement Co. Ltd. (Anhui Province, China). The average particle size of the silica fume (SF) used was 0.1–0.3 μm , and the specific surface area was 25,000 m^2/kg . Quartz powder and quartz sand (QS) were used as aggregates with an apparent density of 2,650 kg/m^3 . A polycarboxylic acid high-efficiency water reducing agent (SP) with a solid content of 40% and a water reduction rate >40% was used to meet the flowability requirements. Magnesite was obtained from Haicheng, Liaoning, China, in the form of white lumps. The $MgCO_3$ content is up to 94%.

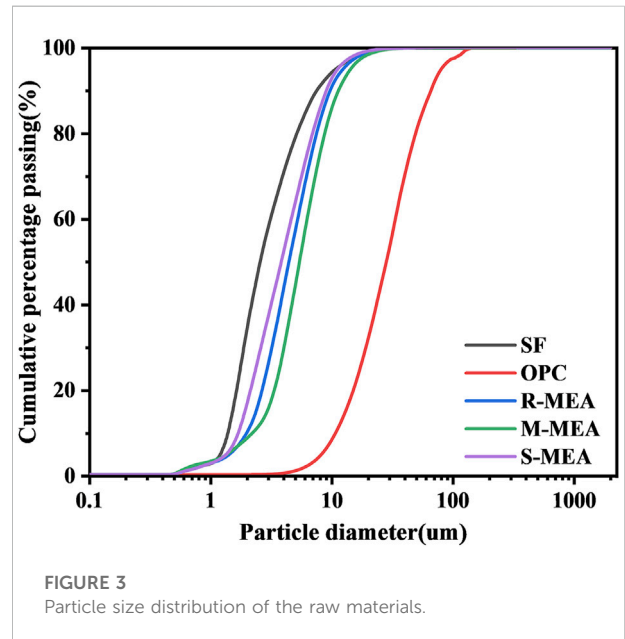
MEA was prepared by calcination of magnesite at calcination temperatures/holding times of 750°C/1.5 h, 950°C/2 h and 1,000°C/2 h. MEAs with different reactivity are denoted as R-MEA (Rapid reactivity), M-MEA (Medium reactivity) and S-MEA (Slow reactivity). According to Chinese standard T/CCPA 5-2017, the citric acid neutralization reaction was used to determine the active reaction time of MEA, with a short neutralization time implying high activity. The activity values at 41 s, 105 s and 213 s were determined by citric acid neutralization reaction. The main chemical compositions of the raw materials are shown in Table 1. The XRD patterns of the different active MEAs are shown in Figure 1. It was observed that the R-MEA crystal structure was relaxed, with many lattice distortions and defects, and offered promising activity in the hydration reaction. The R-MEA diffraction peaks contain $MgCO_3$ peaks, which may be due to insufficient calcination

TABLE 1 Main chemical composition of raw materials (wt%).

Oxide	MgO	Na ₂ O	Al ₂ O ₃	SiO ₂	P ₂ O ₅	K ₂ O	CaO	Fe ₂ O ₃	LOI
OPC	2	0.14	5.4	17.83	0.1	6.22	60.31	7.22	0.78
SF	0.84	0.16	0.48	96.21	0.03	0.03	0.4	-	1.85



temperature and/or holding time. However, it still has the highest reactivity compared to the other two expansion agents, according to the citric acid neutralization reaction. In contrast, the M-MEA



and S-MEA had dense structures and complete lattices, showing sequentially lower activity.

The SEM image in Figure 2 also provides a visual characterization of the above results. It also shows that as the sintering temperature increases, the MEA gradually becomes denser and the internal pores gradually decrease in number

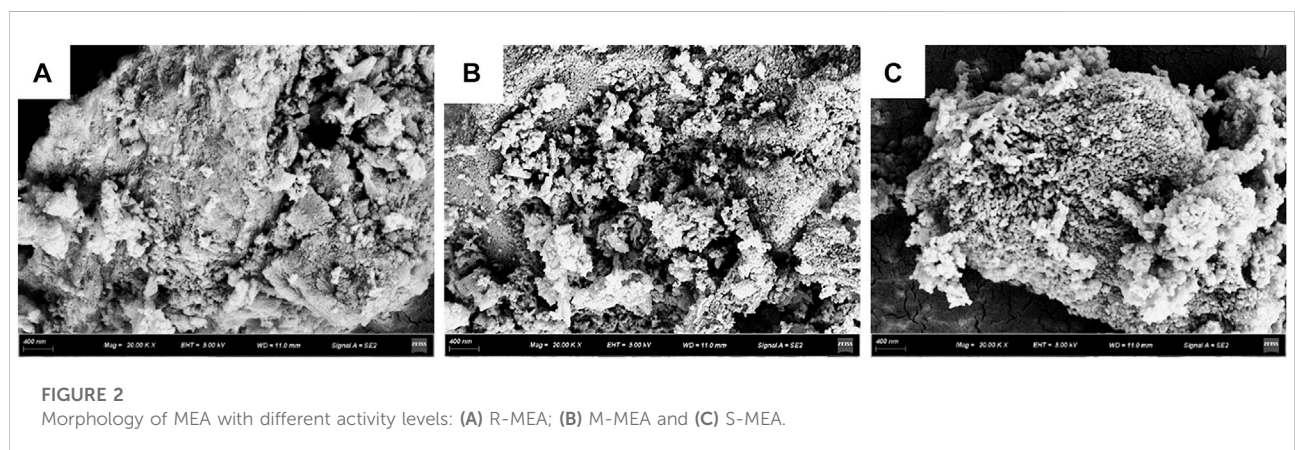


TABLE 2 Mix proportions of the test (kg/m³).

ID	OPC	SF	QS	SP	R-MEA	M-MEA	S-MEA
C-0.18	850	150	1,250	20	-	-	-
R3-0.18	820	150	1,250	20	30	-	-
R6-0.18	790	150	1,250	20	60	-	-
R9-0.18	760	150	1,250	20	90	-	-
R6-0.16	790	150	1,250	20	60	-	-
R6-0.20	790	150	1,250	20	60	-	-
M6-0.18	790	150	1,250	20	-	60	-
S6-0.18	790	150	1,250	20	-	-	60

which means that the chance of moisture intrusion from the internal pores during the hydration reaction is lessened.

The particle size distributions of these binder materials are shown in Figure 3. It can be seen that the particle size distributions of the three expansion agents are between those of SF and OPC, while S-MEA has a relatively small particle size.

2.2 Sample preparation

The concrete compound used for autogenous shrinkage and mechanical property characterisation experiments is shown in Table 2. The UHPC mixing process was as follows: 1) add all powders, quartz sand, and high-efficiency water-reducing agent to the mixer and mix for 1 min; 2) add water, slowly mix for 5 min and, finally, rapidly mix for 1 min; 3) load the fresh concrete into

moulds for testing. The samples did not contain steel fibre, which could influence the test results.

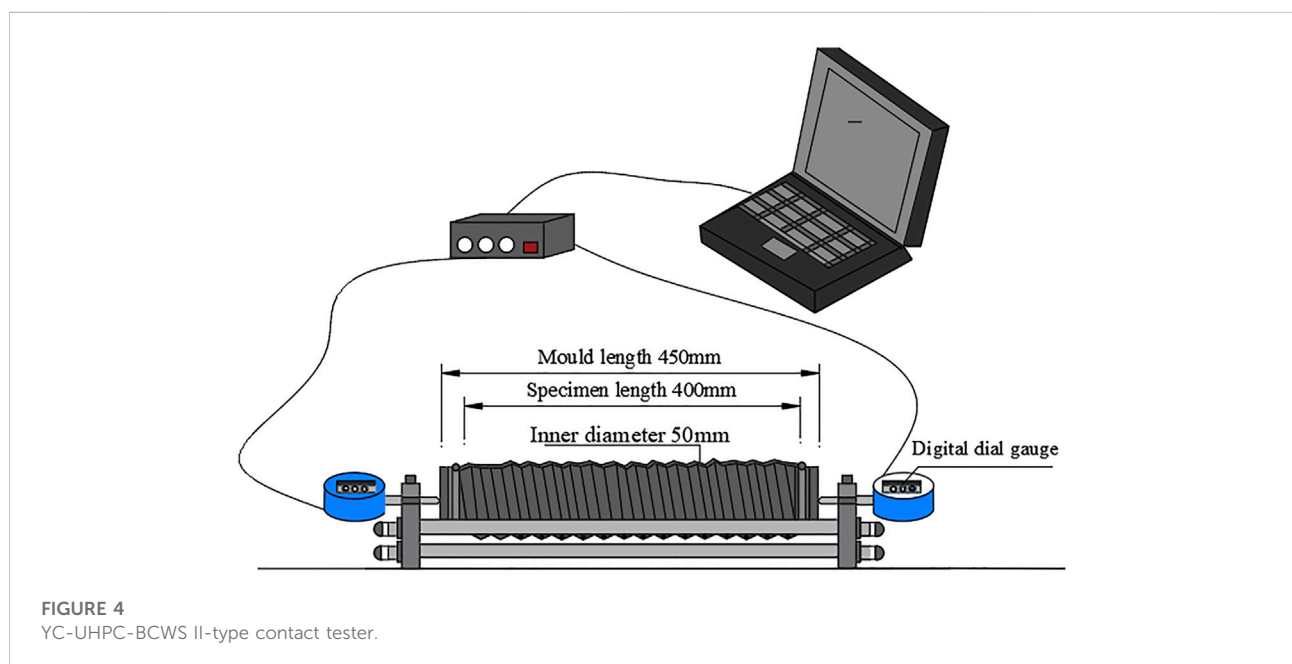
3 Methods

3.1 Mechanical properties

The prisms were demoulded approximately 24 h after casting. After curing for 3, 7, and 28 d, the flexural and compressive strengths of the specimens were tested according to standard BS EN 196-1, by using cubic samples (40 mm³ × 40 mm³ × 40 mm³). At least three specimens were tested at each age to compute the average strength.

3.2 Autogenous deformation

The tests used a YC-UHPC-BCWS II-type contact tester in Figure 4 to determine the autogenous shrinkage of UHPC. The bellows was an impermeable steel wire-reinforced polyurethane (PU) hose with an internal diameter of 50 mm and length of 450 mm. A micrometer was used with a resolution of 1 μm and an accuracy >5 μm. The autogenous shrinkage test was conducted at a constant temperature of 20 ± 2°C and a constant humidity of 60 ± 5%. The vibrated and compacted concrete was loaded into a PU hose, placed on a horizontal steel rod holder and stabilized for 10 min, and then the concrete deformation was measured every 30 s. Testing was performed according to ASTM C1698-09, with the difference that we used more than double the standard dial, which doubled the



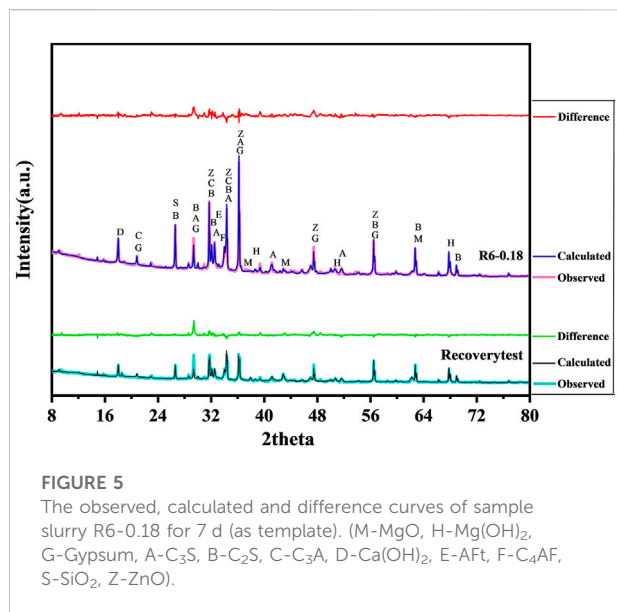


FIGURE 5

The observed, calculated and difference curves of sample slurry R6-0.18 for 7 d (as template). (M-MgO, H-Mg(OH)₂, G-Gypsum, A-C₃S, B-C₂S, C-C₃A, D-Ca(OH)₂, E-AfT, F-C₄AF, S-SiO₂, Z-ZnO).

measurement accuracy. Each sample was tested for three kinds of autogenic deformation, with the average value taken as the final result.

3.3 Heat of hydration

The binder material of each component was first weighed and then mixed well according to Table 2, and then the amounts of water and SP were calculated according to the w/b ratio. After the preheated water and binder material were subsequently mixed well by hand, about 30 g of mixture was quickly put into an eight-channel isothermal calorimeter. The exothermic rate dQ/dt and the exothermic heat Q of the binder material during the hydration reaction were measured uninterruptedly within 7 d.

3.4 X-ray diffraction analysis

After 7 d, the cured samples were removed and broken into small pieces. Intermediate-sized pieces were taken and added to an appropriate amount of anhydrous ethanol, then put into an agate mortar and ground until the particles passed through an 80- μ m square-hole sieve. After evacuation and complete drying, the ZnO that passed through the sieve was added as the internal marker, mixed with the cured sample powder at a ratio of 1:9 (wt %) and then analysed by XRD. Both MgO and Mg(OH)₂ are simple crystals, and their contents were quantified by XRD-Rietveld quantitative analysis using MDI Jade software. Figure 5 shows the observed, calculated and difference curves of sample slurry R6-0.18 cured for 7 d. Based on this template, the contents

TABLE 3 Recovery test.

ID	MgO	Mg(OH) ₂
Raw material (%)	2.8	-
Addition (%)	3.8	2.1
Detection (%)	6.4	2.0
Recovery (%)	96.97%	95.24%

of substances after hydration were calculated in other groups. To ensure the accuracy of the analysis, the fitting factors R were all within 10%.

A recovery test is one way to evaluate the accuracy of the XRD internal standard method (Xu, 2014). Therefore, in the experiment, we added MgO and Mg(OH)₂ pure phases to sample C-0.18 to check the accuracy of the XRD-Rietveld quantitative analysis (Table 3). The recoveries of MgO and Mg(OH)₂ calculated by fitting were 96.97 and 95.24%, respectively, which indicates that the determination of MgO and Mg(OH)₂ by XRD-Rietveld quantitative analysis was feasible.

3.5 Pore structure

A hydrated sample was cut into a cube-shaped sample of about 20 mm, soaked in anhydrous ethanol for 24 h, and dried in a 40°C oven. Then, the independent pores of the samples were detected by mercury intrusion porosimetry (MIP), and the connected pores were detected by X-ray computed tomography (X-CT). X-CT is a non-destructive testing method used to detect micropore development trends inside solid materials such as concrete. The latest research has used multi-mounted X-ray computed tomography that rotates around multiple objects (Fu et al., 2016). Its greatest advantage is that it can visualize fine cracks in the scanned section and make up for the limitation of MIP, which can only evaluate independent pores; i.e. (Liu et al., 2019). The X-CT technique can evaluate independent and connected pores comprehensively. The X-ray tube pressure range was 30–160 KeV with a probe travel range of 290 mm. All independent pores were imaged and reconstructed by 3D visualization. Only the combination of MIP and X-CT allows precise measurement of all pores.

3.6 SEM morphology

Thin slices of cured paste samples of different ages were made, their hydration terminated with anhydrous ethanol, and placed in a vacuum drying oven at 40°C for 12 h. The dried specimens were sprayed with Au for scanning electron microscopy (SEM).

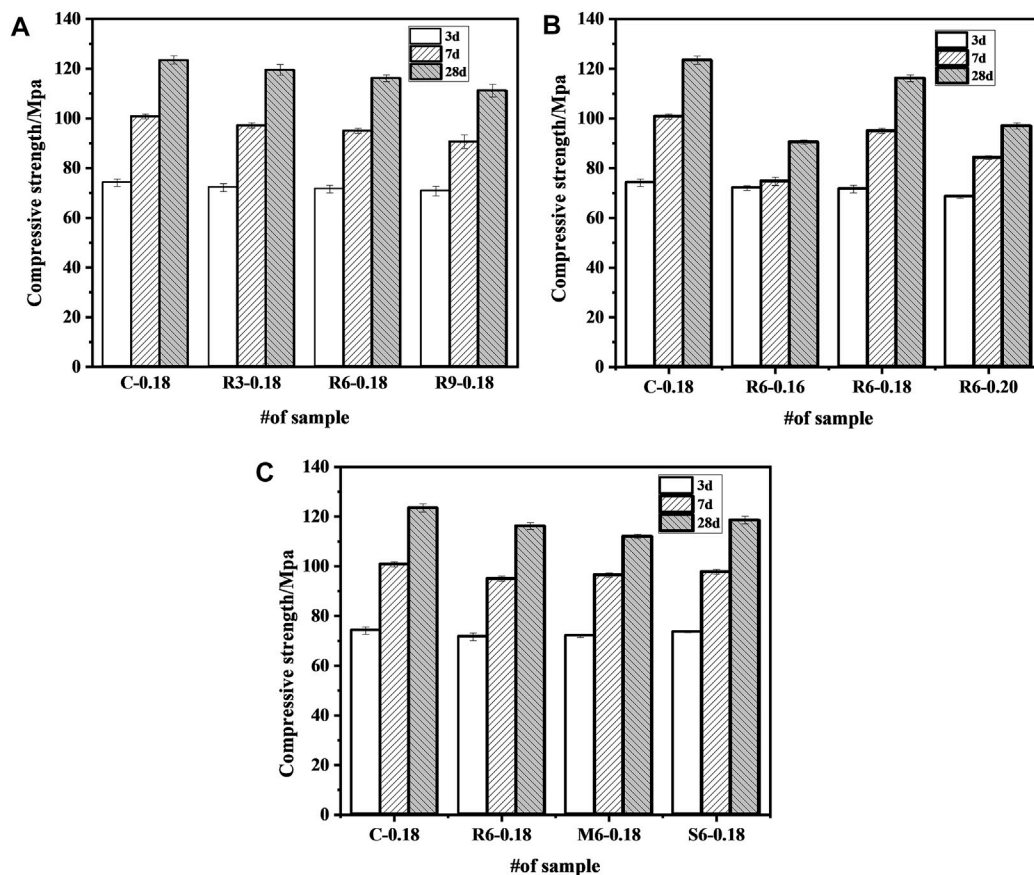


FIGURE 6
Effect of MEA on compressive strength of UHPC (A) content; (B) w/b ratio; (C) activity level.

4 Results and discussion

4.1 Effect of MEA on the compressive strength of UHPC

Figure 6A indicates the effect of MEA content on mechanical properties of UHPC. The mechanical properties of UHPC gradually decrease with the increase of MEA doping. When the addition of R-MEA was increased from 3% to 9%, the mechanical properties of UHPC were eventually reduced by 4 MPa and 12.3 MPa, respectively, relative to the control group. This indicates that the compressive strength of UHPC decreases with the increase dosage of MEA. The reduction mainly due to the fact that MEA has a smaller specific surface area than cement particles, and the hydration reaction occurs more easily than cement particles by obtaining water, which reduces the hydration products of cement. In addition, the mechanical properties of UHPC are reduced by the use of internal mixing method in which some of the cement is replaced by MEA. It should be emphasized that although it

reduces the mechanical properties, the amount of cement is also reduced accordingly, and in addition, carbon dioxide can be collected and used to cure MgO-based cement (Mo et al., 2014), producing a more environmentally friendly UHPC.

Figure 6B shows the effect of different w/b ratios on the compressive strength of UHPC. At w/b ratios of 0.16, 0.18, and 0.20, the compressive strength of UHPC samples at 28 d was reduced by 33 MPa, 7.3 MPa, and 26.5 MPa, respectively, compared to the control group. Compared to a w/b ratio of 0.18, increasing or decreasing the w/b ratio will reduce the compressive strength. A too-low w/b ratio had a more significant effect. The result is may different from that of ordinary concrete (Sanawung et al., 2017), which mainly attributed to the fact that UHPC contains a large amount of cementitious material, and with a very low w/b ratio, a significant portion of cement cannot be hydrated, as also seen from the diffraction peak of C_3S in Figure 5. If the w/b ratio continues to decrease, the unhydrated cement particles will increase, leading to a decrease in the compressive strength of UHPC. A w/b ratio of 0.20 reduced the compressive strength of the specimen. The

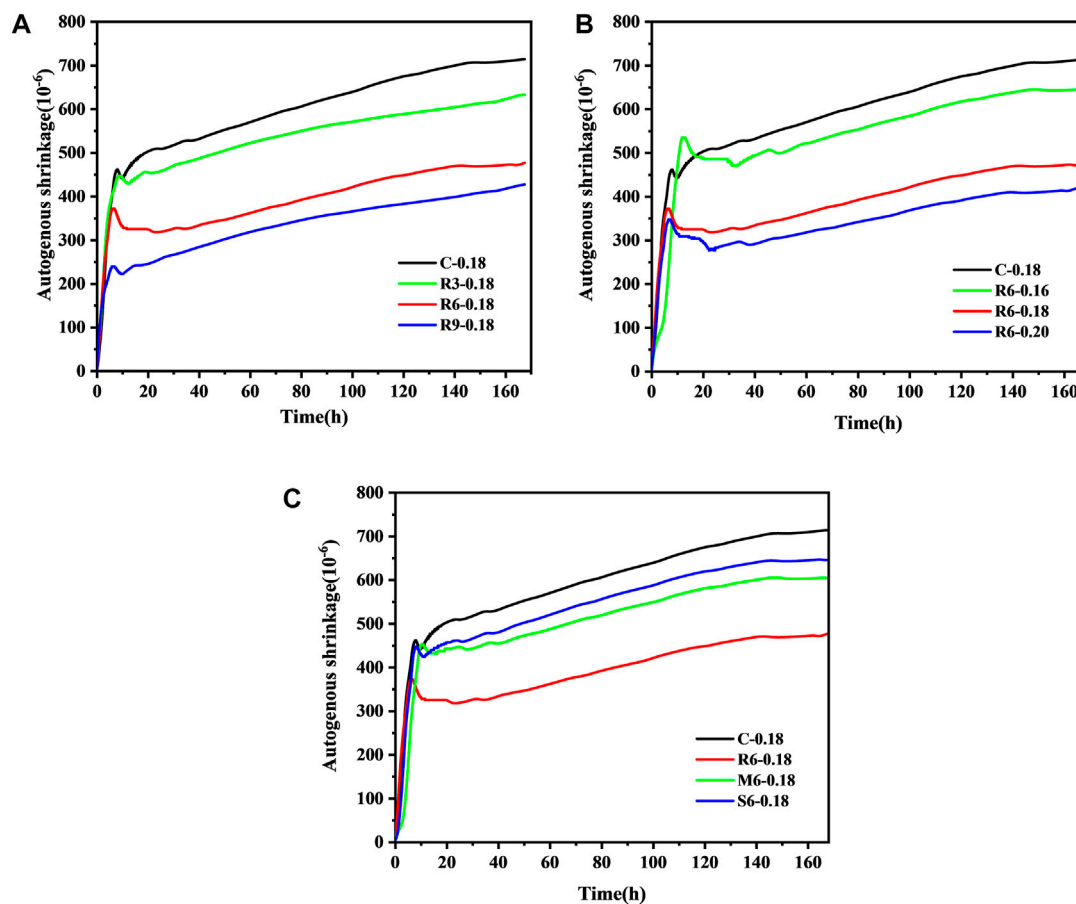


FIGURE 7 Effect of MEA on the autogenous shrinkage performance of UHPC (A) content; (B) w/b ratio; (C) activity level.

possible reason is that the space originally filled by cementitious material was filled with water (Du et al., 2021), which led to a reduction in early compressive strength.

Figure 6C shows the effect of different active MEAs on the compressive strength of UHPC. Compared with the control group, the compressive strength at 28 d was reduced by 7.3 MPa, 11.5 MPa, and 4.9 MPa after incorporating 6% R-MEA, M-MEA, and S-MEA, respectively. The results show that MEA with different activity levels all reduced the compressive strength of UHPC, which mainly due to the hydration products of MEA do not contribute as much to compressive strength as cement (Li, 2012). Both M-MEA and S-MEA had higher compressive strengths than R-MEA. The possible reason is that R-MEA has lower crystallinity, more defects, and a larger specific surface area, which makes it easier to obtain water in competition with cement hydration, thus resulting in less water being required for cement hydration, the generation of fewer hydration products, and reduced mechanical properties.

4.2 Effect of MEA on the autogenous shrinkage of UHPC

Figure 7A shows the effect of MEA content on the autogenous shrinkage of UHPC. Figure 7B shows the effect of the w/b ratio on the autogenous shrinkage of UHPC, while Figure 7C shows the impact of MEA with different activity levels on the autogenous shrinkage of UHPC.

As shown in Figure 7A, the autogenous shrinkage of control group at 168 h attained 713.66 $\mu\epsilon$. The amount of MEA doping had a significant effect on the autogenous shrinkage of UHPC. It should be noticed that all samples have a slow expansion process at about 5 h–7 h and then shrink at a faster rate. The incorporation of MEA does not change the shrinkage trajectory of UHPC. Finally, the autogenous shrinkage of the corresponding UHPC was reduced by 11.41%, 33.32%, and 40.28% at 168 h for R-MEA contents of 3%, 6%, and 9%, respectively.

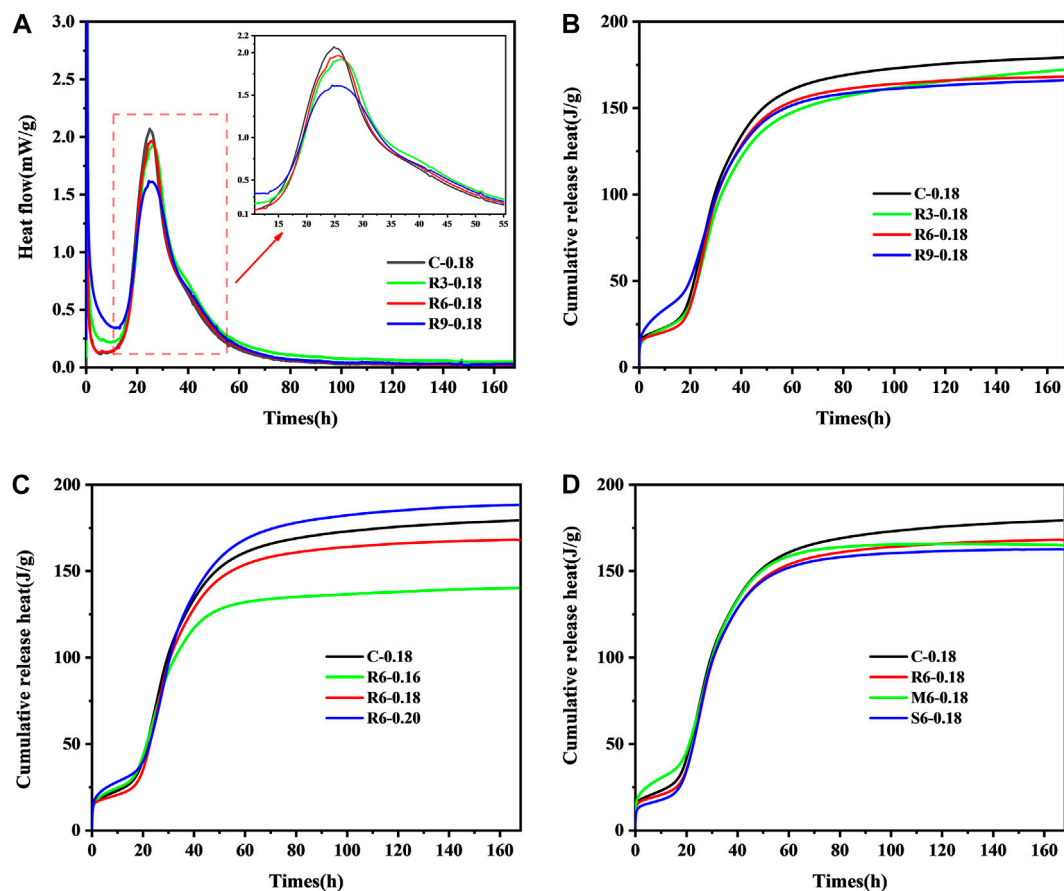


FIGURE 8

Effect of MEA content on (A) heat flow rate; (B) cumulative heat release rate of UHPC pastes, and effect on cumulative heat release rate (C) w/b ratio, (D) activity level.

From Figure 7B, it can be found that the autogenous shrinkage of the corresponding UHPC was reduced by 9.63%, 33.32%, and 41.18% at 7 d with w/b ratios of 0.16, 0.18, and 0.2, respectively. This indicates that the higher the water content during mixing, the more effective MEA is in reducing the shrinkage of UHPC. The reason for this is that a high w/b ratio allows MEA to capture free water in competition with the cementitious material, making the MEA hydration reaction more complete. Deng et al. (Deng, 1990) concluded that the fine $Mg(OH)_2$ clustered near the MgO particles can produce larger expansion, and the coarse $Mg(OH)_2$ dispersed in the larger area around the MgO particles cause less expansion. It should be emphasized that when the w/b ratio of ordinary concrete is high, Mg^{2+} can readily diffuse to a position relatively far from MgO particles, resulting in a slight expansion. In contrast, the expansion of MEA in UHPC increases with the w/b ratio, which may be attributed to its meagre w/b ratio and high viscosity, which are

insufficient to allow Mg^{2+} to diffuse readily. Recent studies have also shown that highly active MEAs are more sensitive to relative humidity (RH) than less active ones. Thus, a larger w/b ratio is more conducive to the micro-expansion of R-MEA (Wang et al., 2022).

As shown in Figure 7C, the autogenous shrinkage of the UHPC matrix was reduced by 33.32%, 15.42%, and 9.59% by doping with 6% R-MEA, M-MEA, and S-MEA, respectively. Therefore, MEA can effectively reduce the early autogenous shrinkage of UHPC and, the higher the activity, the more pronounced the compensating shrinkage effect. However, even the highest R-MEA activity is still not enough to account for the complete shrinkage of UHPC because the specimens still show shrinkage on a macroscopic scale. Combined with Figure 7, it is clear that the effect of w/b ratio on the MEA-UHPC system is greater than that of MEA activity level, since 6% M-MEA at w/b ratio = 0.18 reduces shrinkage almost as effectively as R-MEA at w/b ratio = 0.16.

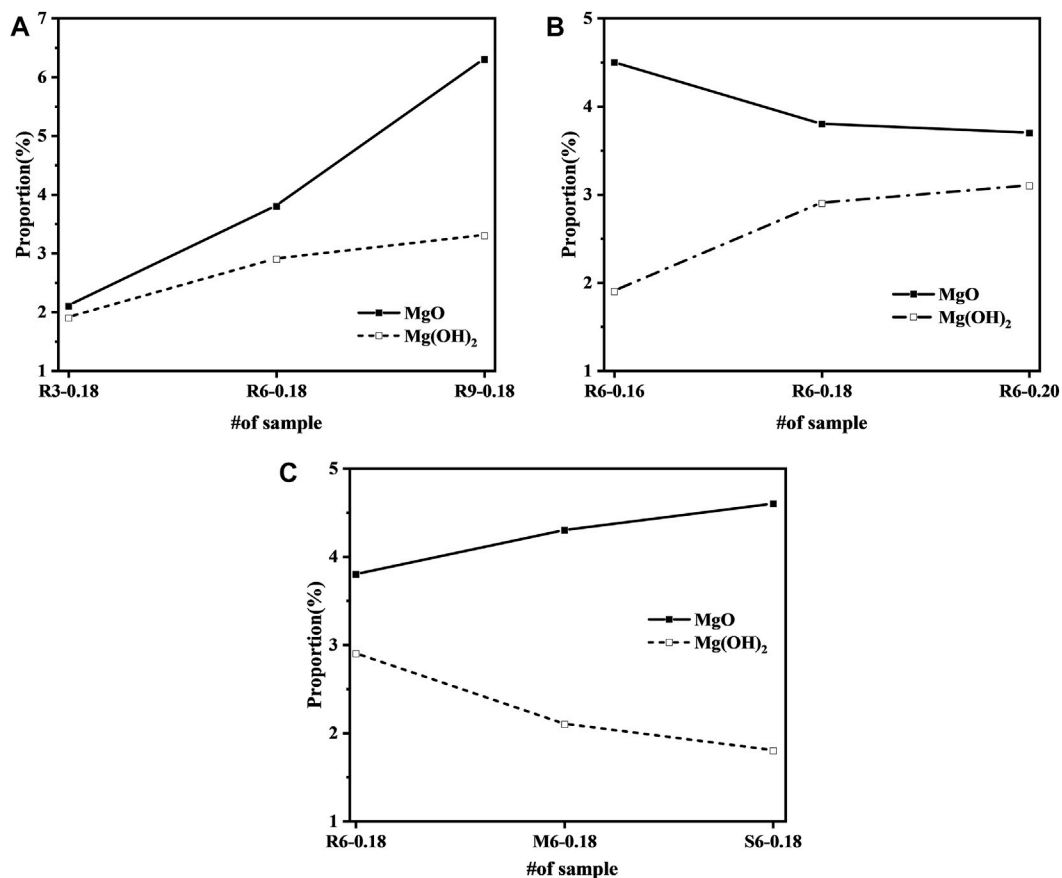


FIGURE 9 Effect of MEA hydration products on UHPC (A) content; (B) w/b ratio, (C) activity level.

4.3 Effect of MEA on the heat of hydration

From Figure 8A, It can be observed that the UHPC induction period is extended, generally being close to 11 h, which may be related to the slow dissolution of cement particles at low w/b ratios. That is, the surfaces of the cement particles are covered by hydrated calcium silicate gel, which essentially hinders the hydration reaction process. After the induction period, the acceleration period begins, which lasts for about 12 h. At this stage, the expansion effect caused by the heat of cement hydration is greater than its shrinkage effect, which is manifested as micro-expansion on the autogenous shrinkage graph. Then, the cement hydration process enters the period of stabilization.

Figure 8B shows the effect of MEA incorporation on the cumulative heat release. The cumulative heat release of UHPC decreases with the increase of MEA incorporation, which is due

to the fact that the exotherm of MgO hydration is less than that of cement.

Figure 8C shows that a lower w/b ratio decreases the cumulative heat release rate of the UHPC paste, which is mainly caused by the incomplete hydration of cement particles. It can be seen that cement hydration can be fully completed at w/b ratio = 0.2, and the accumulated heat release rate is even higher than that of the control group. There is no doubt that the increase in internal temperature will contribute to the further expansion of MEA, which is also one of the reasons for the better compensation shrinkage seen in sample R6-0.20 according to Figure 7B.

Figure 8D shows that the addition of all types of MEA reduces the cumulative heat release of UHPC paste. The lower the activity level, the more pronounced the effect is, which indicates that the high-activity MgO contributes more to the heat flow of the paste during hydration.

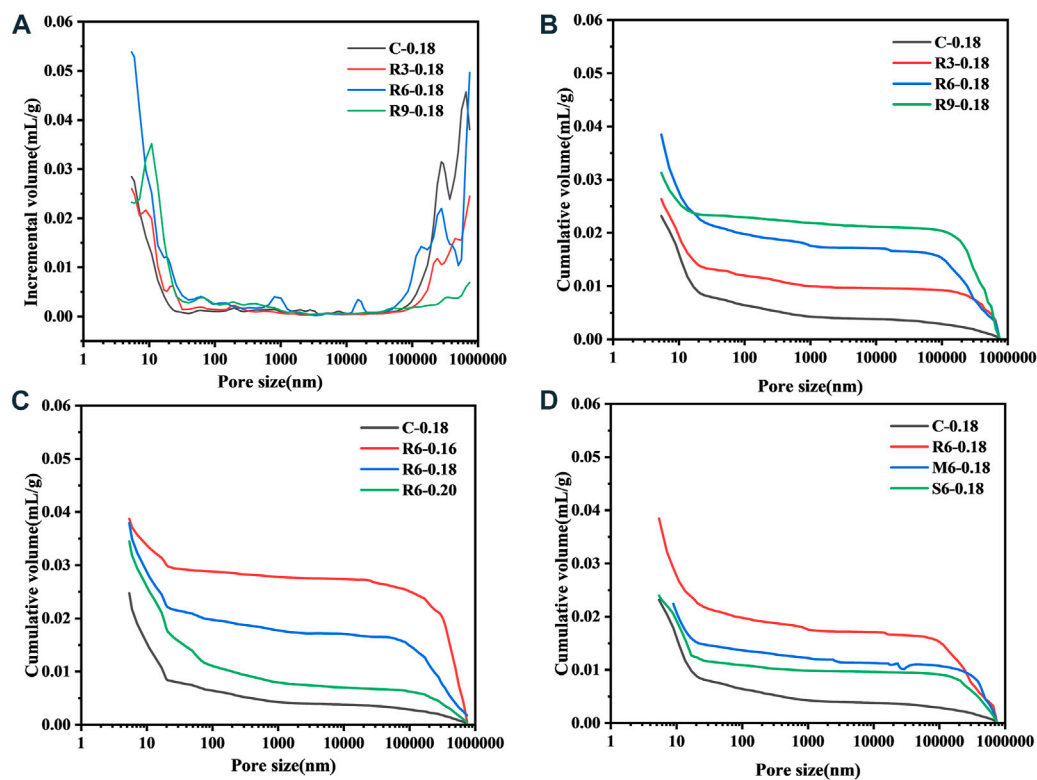


FIGURE 10 Effect of MEA activity level and w/b ratio on the connected pores (A) volume increment, (B) cumulative volume.

4.4 Effect of MEA hydration products on UHPC

The MgO and Mg(OH)₂ contents in each cement paste as measured by XRD-Rietveld quantitative analysis are shown in Figure 9. From Figure 9A, it can be seen that the content of Mg(OH)₂ is positively correlated with MEA, but not in a simple linear relationship. Compared with the doping level of 3%, when the content was increased to 6% and 9%, the hydration reaction produced 1.33 and 1.11 times higher MH, respectively, which is in general agreement with the compensated autogenous shrinkage rate in Figure 7. From Figure 9B, it can be seen the content of Mg(OH)₂ increases with the w/b ratio. Meanwhile, Figure 9C indicates that the higher the reactivity, the more fully hydrated the MEA is. This indicates that the hydration of MgO is limited by the water in the slurry, and sufficient water is beneficial to the secondary crystallization of Mg(OH)₂, which generates higher crystal growth pressure and promotes expansion of the mortar. It can also be seen that even if the w/b ratio is increased to 0.20, the MEA will not be fully hydrated after 7 d and minor swelling continues.

4.5 Pore structure

4.5.1 Mercury intrusion porosimetry

Figure 10 shows the changes in the connected pore structure after incorporation of MEA with different reactivity levels into the UHPC (7 d). From Figure 10A, it can be seen that after MEA incorporation, the pore size of the UHPC is mainly distributed in the ranges of 5–50 nm and 100–780 nm. In cementitious materials, pores smaller than 50 nm are closely related to autogenous shrinkage (Shah, et al., 1992). R-MEA essentially increases the sizes of pores <50 nm in the UHPC, which is beneficial in reducing its early shrinkage and is consistent with previous observations (Li et al., 2021). From Figures 10B–D, it can be seen that the porosity of the cumulative connected pores increases gradually with the increase of R-MEA doping. In fact, as can be seen in Figure 10, the porosity of the UHPC connected pores all increased with the addition of MEA and increased more significantly with the decrease of the w/b ratio.

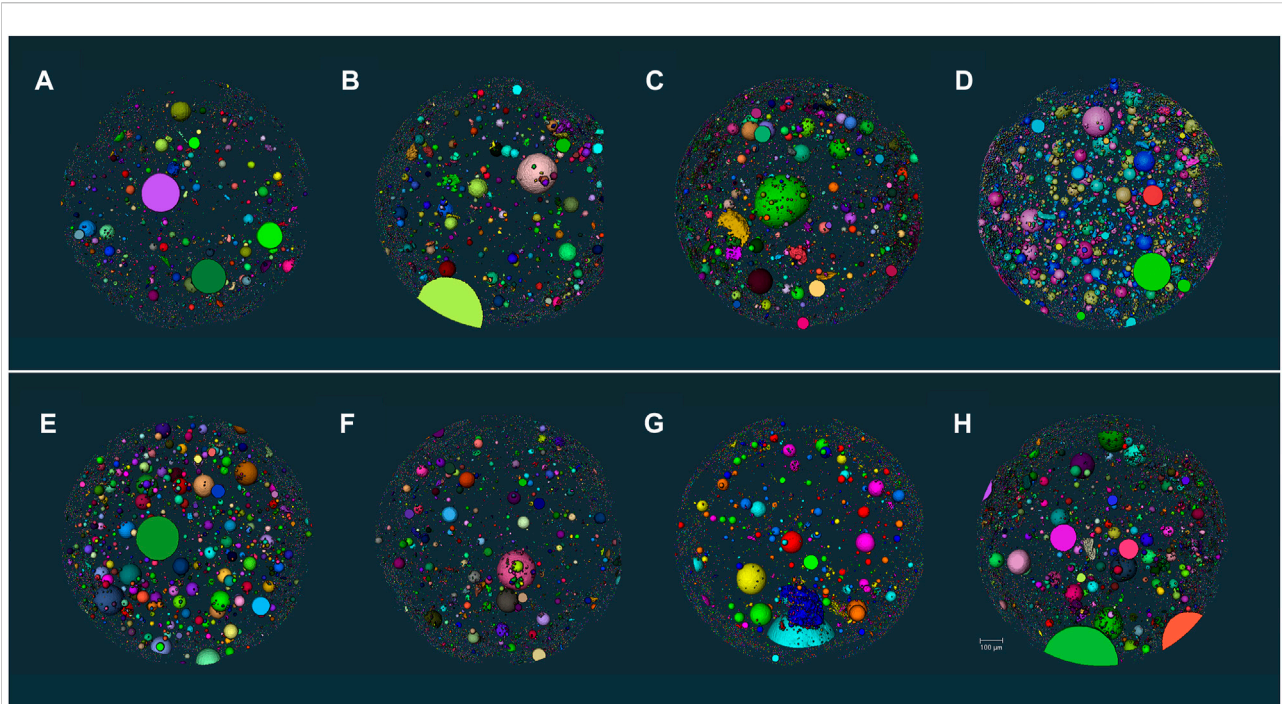


FIGURE 11
3D visualization (A) C-0.18, (B) R3-0.16, (C) R6-0.18, (D) R9-0.18, (E) R6-0.16, (F) R6-0.20, (G) M6-0.18, (H) S6-0.18.

TABLE 4 Effect of w/b ratio and activity level of MEA on the porosity of UHPC.

ID	Connected porosity (%)	Independent porosity (%)	Total porosity (%)
C-0.18	5.697	1.369	7.066
R3-0.18	5.087	2.508	7.595
R6-0.18	8.596	3.139	11.735
R9-0.18	8.604	3.346	11.950
R6-0.16	7.026	3.802	10.828
R6-0.2	5.438	1.898	7.335
M6-0.18	7.843	2.808	10.651
S6-0.18	7.052	3.273	10.325

4.5.2 X-ray computed tomography

The X-CT analysis focused more on the distribution of pores $>1\ \mu\text{m}$ (Aligizaki, 2005). Figure 11 shows the 3D reconstruction of the sample. The total porosity of each sample is summarized in Table 4 after MIP tests for independent pores and X-CT analysis for connected and independent pores. It shows that the addition of MEA increases the porosity of UHPC, while the addition of R-MEA leads to the most rapid increase in porosity. The direct driving force for the swelling of MEA comes from the swelling force and crystallization pressure of $\text{Mg}(\text{OH})_2$ (José et al., 2020), which is the hydration product of MEA. This causes the pores in the

matrix to expand. Based on the results of XRD tests, it appears that R-MEA is more likely to produce a large number of $\text{Mg}(\text{OH})_2$ crystals, resulting in a higher crystallization pressure and a matrix with greater porosity.

It can also be found that the porosity was reduced by 32.26% at w/b ratio = 0.2 compared to w/b ratio = 0.16. This indicates that increasing the w/b ratio decreases the porosity of UHPC. The main reason is that a low w/b ratio reduces the cement hydration rate, so the cement hydration reaction lacks sufficient water to generate enough hydration products to fill the pore structure, leading to an increase in the number of harmful pores.

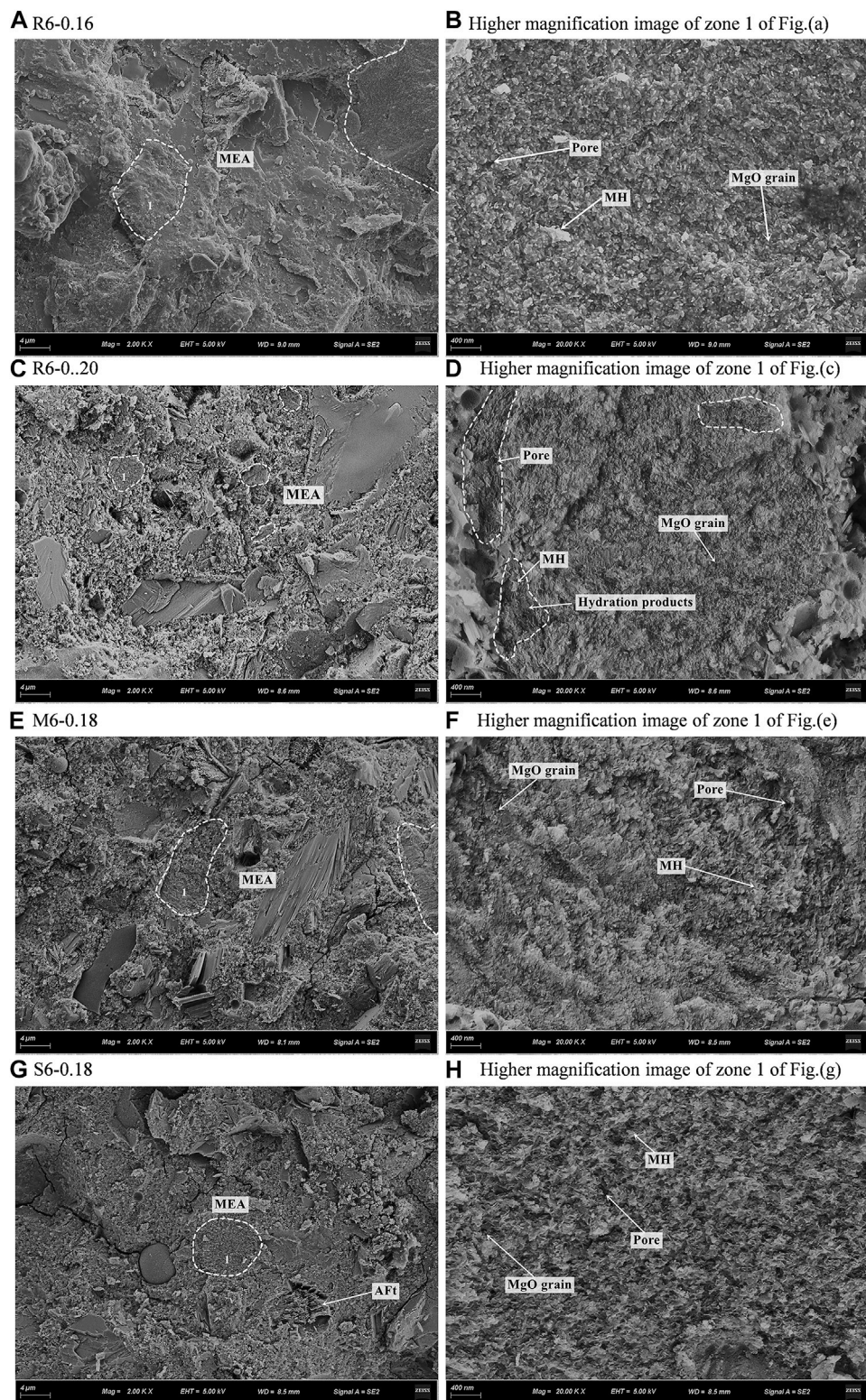


FIGURE 12
The microscopic morphology of the cement paste after incorporation of MEA (7 d).

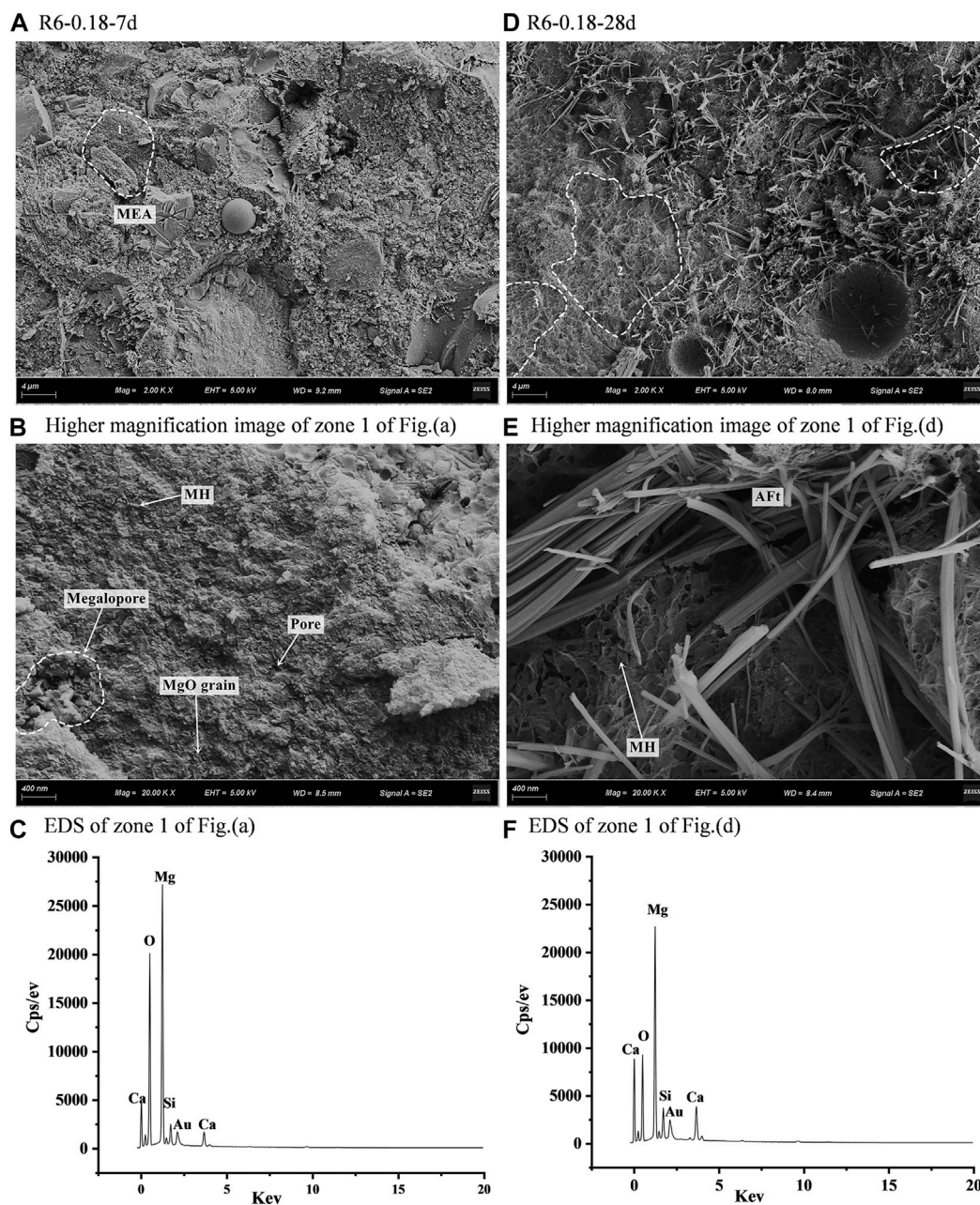


FIGURE 13
The morphology of R6-0.18 hydration products at the age of 7 d and 28 d.

4.6 Morphology

Figure 12 shows the microscopic morphology of the cement paste after incorporation of MEA (after 7 d). It can be observed that all MEAs undergo hydration reactions in a restricted area, which is an essential reason for their swelling. Figure 12B shows a paste sample with w/b ratio = 0.2. Compared to the R6-0.16 specimens (Figure 12A), due to the presence of more water, the MgO particles,

which are at the edges of the MEA, are more hydrated because of the lower ion concentration, while the R-MEA is also penetrated by the hydration products of the cement and is hydrated in many places, producing more extensive swelling. More ettringite (AFt) is evident in Figure 11D compared to the other two expansion agents (Figure 12F and Figure 12H). This may be related to the low activity of S-MEA, which does not compete with cement for water as much as R-MEA does. This is one of the reasons why

UHPC exhibits greater strength when mixed with the same dose of S-MEA. It can also be seen in Figure 11 that the $\text{Mg}(\text{OH})_2$ crystals grow in a scaffold-like manner, while the curing of the highly bonded slurry and $\text{Mg}(\text{OH})_2$ crystals leads to swelling (Cao and Yan, 2019). However, the MEA hydration products are not regular, which may be related to the effect of the alkaline environment generated by the cementitious material on $\text{Mg}(\text{OH})_2$ (Lv, et al., 2004).

Figure 13 shows the microscopic morphology of sample R6-0.18 after hydration at different ages. It can be seen that R-MEA increases the porosity of UHPC to a more considerable extent. A high aggregation of MgO grains in the UHPC can be observed at 28 d and a higher amount of $\text{Mg}(\text{OH})_2$ is produced, resulting in swelling. In the UHPC at the age of 28 d (Figure 13A), the boundary between the MEA hydration products and cementitious material in regions 2 and 3 becomes blurred (Figure 13D); i.e., the hydration products of the cementitious material and MEA are symbiotic. As the age increases, the rod-shaped ettringite particles cross each other and penetrate the $\text{Mg}(\text{OH})_2$ (Figure 13E and Figure 13F), making the MEA hydration products and cement substrate further strengthen the binding ability.

5 Conclusion

The effects of MEA with different w/b ratios and activity levels on the mechanical properties, shrinkage deformation and microstructure of UHPC were investigated in this paper. The main findings are as follows.

- 1) Adding MEA to UHPC reduces its compressive strength. The higher the MEA activity level, the more pronounced the reduction. However, MEA can effectively mitigate the autogenous shrinkage of UHPC, with R-MEA having the greatest apparent effect on reducing UHPC shrinkage. Considering the mechanical properties and shrinkage-reducing effect, it is recommended to use M-MEA to formulate UHPC that can minimize shrinkage. The compressive strength of the specimens containing 6% of M-MEA decreased by 9.31%, while the autogenous shrinkage of UHPC decreased by 15.42%.
- 2) The combination of MIP and X-CT analyses can effectively measure the porosity of concrete. This showed that MEA increases the porosity of UHPC, with R-MEA providing the greatest increase. The samples containing 3%, 6%, and 9% R-MEA increased the UHPC porosity by 0.53%, 4.67%, and 4.88%, respectively.
- 3) The accuracy of XRD-Rietveld quantitative analysis can be confirmed by a recovery test. The higher the activity and w/b ratio, the more $\text{Mg}(\text{OH})_2$ is produced after the MEA hydration reaction, as measured by the quantitative analysis.
- 4) The w/b ratio has a significant impact on the performance of UHPC. The results showed that the UHPC specimens with w/b ratio = 0.18 had the greatest compressive strength

compared to the w/b ratios of 0.16 and 0.20. The more $\text{Mg}(\text{OH})_2$ produced by the hydration reaction of MEA can better compensate for the autogenous shrinkage of UHPC, and it is also beneficial to reduce the porosity, by increasing the w/b ratio. However, at low w/b ratios, there are fewer MEA hydration products and the expansion force is insufficient

Data availability statement

The original contributions presented in the study are included in the article/Supplementary Material, further inquiries can be directed to the corresponding authors.

Author contributions

ZZ designed the experiments and wrote the manuscript. ZZ, SL, PC, XL, and JW performed the experiments and contributed to the discussion part. XL and JW processed data and made charts. SL and PC did the review and editing, and contributed to the discussion part. All authors contributed to the article and approved the submitted version.

Funding

This research was financially supported by the GuangXi Key Laboratory of New Energy and Building Energy Saving of China (No.22-J-21-24).

Acknowledgments

The authors would like to thank Prof. TaiChao Su of Guilin University of Technology for his review of the paper.

Conflict of interest

The authors declare that the research was conducted in the absence of any commercial or financial relationships that could be construed as a potential conflict of interest.

Publisher's note

All claims expressed in this article are solely those of the authors and do not necessarily represent those of their affiliated organizations, or those of the publisher, the editors and the reviewers. Any product that may be evaluated in this article, or claim that may be made by its manufacturer, is not guaranteed or endorsed by the publisher.

References

- Aligizaki, K. K. (2005). *Pore structure of cement-based materials: Testing, interpretation and requirements*. Boca Raton: CRC Press.
- Cao, F., and Yan, P. (2019). The influence of the hydration procedure of MgO expansive agent on the expansive behavior of shrinkage-compensating mortar. *Constr. Build. Mater.* 202, 162–168. doi:10.1016/j.conbuildmat.2019.01.016
- Cao, F., Miao, M., and Yan, P. (2018). Effects of reactivity of MgO expansive agent on its performance in cement-based materials and an improvement of the evaluating method of MEA reactivity. *Constr. Build. Mater.* 187, 257–266. doi:10.1016/j.conbuildmat.2018.07.198
- Chatterji, S. (1995). Mechanism of expansion of concrete due to the presence of dead-burnt CaO and MgO. *Cem. Concr. Res.* 25 (1), 51–56. doi:10.1016/00088846(94)00111-b
- Chen, B. C. (2018). Review of ultra-high performance concrete shrinkage. *J. Traffic Transp. Eng.* 18 (1), 13–28. (in Chinese). doi:10.19818/j.cnki.1671-1637.2018.01.002
- Choi, S. W., Jang, B. S., and Lee, K. M. (2013). Fundamental properties of fly ash concrete containing lightly burnt MgO Powder. *J. Korean Soc. Civ. Eng.* 33 (2), 475–481. doi:10.12652/Ksce.2013.33.2.475
- Choi, S., Jang, B. s., Kim, J. h., and Lee, K. m. (2014). Durability characteristics of fly ash concrete containing lightly-burnt MgO. *Constr. Build. Mater.* 58, 77–84. doi:10.1016/j.conbuildmat.2014.01.080
- Dang, J., Zhao, J., and Du, Z. (2017). Effect of superabsorbent polymer on the properties of concrete. *Polymers* 9 (12), 672. doi:10.3390/polym9120672
- Deng, M. (1990). The expansion mechanism of MgO in cement. *J. Nanjing Inst. Chem. Technol.* 12 (4), 11. (in Chinese).
- Du, J., Meng, W., Khayat, K. H., Bao, Y., Guo, P., Lyu, Z., et al. (2021). New development of ultra-high-performance concrete (UHPC). *Compos. Part B Eng.* 224 (9), 109220. doi:10.1016/j.compositesb.2021.109220
- Fu, J., Liu, Z., and Wang, J. (2016). Multi-mounted X-ray computed tomography. *Plos One* 11 (4), e0153406. doi:10.1371/journal.pone.0153406
- José, N., Ahmed, H., Bravo, M., Evangelista, L., and de Brito, J. (2020). Magnesia (MgO) production and characterization, and its influence on the performance of cementitious materials: A review. *Materials* 13 (21), 4752. doi:10.3390/ma13214752
- Juenger, M., and Siddique, R. (2016). Recent advances in understanding the role of supplementary cementitious materials in concrete. *Cem. Concr. Res.* 78, 71–80. doi:10.1016/j.cemconres.2015.03.018
- Kong, X., and Zhang, Z. (2013). Effect of super-absorbent polymer on pore structure of hardened cement paste in high-strength concrete. *J. Chin. Ceram. Soc.* 41 (11), 1474–1480. doi:10.7521/j.issn.0454-5648.2013.11.03
- Kong, X., and Zhang, Z. (2014). Shrinkage reducing mechanism of superabsorbent polymer in high strength concrete. *J. Chin. Ceram. Soc.* 42 (2), 150–155. doi:10.7521/j.issn.04545648.2014.02.4
- Li, Y. B. (2012). Strength and expansive stresses of concrete with MgO-Type expansive agent under restrain conditions. *J. Build. Mater.* 15 (4), 446–450. doi:10.3969/j.issn.1007-9629.2012.04.002
- Li, J., Wu, Z., Shi, C., Yuan, Q., and Zhang, Z. (2020). Durability of ultra-high performance concrete: A review. *Constr. Build. Mater.* 255, 119296. doi:10.1016/j.conbuildmat.2020.119296
- Li, S., Cheng, S., Mo, L., and Deng, M. (2020). Effects of steel slag powder and expansive agent on the properties of ultra-high performance concrete (UHPC): Based on a case study. *Materials* 13 (3), 683. doi:10.3390/ma13030683
- Li, S., Mo, L., Deng, M., and Cheng, S. (2021). Mitigation on the autogenous shrinkage of ultra-high performance concrete via using MgO expansive agent. *Constr. Build. Mater.* 312, 125422. doi:10.1016/j.conbuildmat.2021.125422
- Liu, K., Yu, R., Shui, Z., Li, X., Guo, C., Yu, B., et al. (2019). Optimization of autogenous shrinkage and microstructure for Ultra-High Performance Concrete (UHPC) based on appropriate application of porous pumice. *Constr. Build. Mater.* 214 (30), 369–381. doi:10.1016/j.conbuildmat.2019.04.089
- Liu, A., Fang, Z., Huang, Z., and Wu, Y. (2022). Solving shrinkage problem of ultra-high-performance concrete by a combined use of expansive agent, super absorbent polymer, and shrinkage-reducing agent. *Compos. Part B Eng.* 230, 109503. doi:10.1016/j.compositesb.2021.109503
- Lv, J., Qiu, L., and Qu, B. (2004). Controlled growth of three morphological structures of magnesium hydroxide nanoparticles by wet precipitation method. *J. Cryst. Growth* 267 (3–4), 676–684. doi:10.1016/j.jcrysgro.2004.04.034
- Mehta, P. K. (1973). Mechanism of expansion associated with ettringite formation. *Cem. Concr. Res.* 3 (1), 1–6. doi:10.1016/0008-8846(73)90056-2
- Mo, L., Deng, M., Tang, M., and Al-Tabbaa, A. (2014). MgO expansive cement and concrete in China: Past, present and future. *Cem. Concr. Res.* 57, 1–12. doi:10.1016/j.cemconres.2013.12.007
- Richard, P., and Cheyrezy, M. (1995). Composition of reactive powder concretes. *Cem. Concr. Res.* 25 (7), 1501–1511. doi:10.1016/0008-8846(95)00144-2
- Ruan, S., and Unluer, C. (2016). Comparative life cycle assessment of reactive MgO and Portland cement production. *J. Clean. Prod.* 137 (20), 258–273. doi:10.1016/j.jclepro.2016.07.071
- Sanawung, W., Cheewaket, T., Tangchirapat, W., and Jaturapitakkul, C. (2017). Influence of palm oil fuel ash and W/B ratios on compressive strength, water permeability, and chloride resistance of concrete. *Adv. Mater. Sci. Eng.* 9, 1–8. doi:10.1155/2017/4927640
- Shah, S. P., Karaguler, M. E., and Sarigaphuti, M. (1992). Effects of shrinkage-reducing admixtures on restrained shrinkage cracking of concrete. *Ac Mater. J.* 89 (3), 289–295. doi:10.14359/2593
- Shen, P., Lu, L., He, Y., Wang, F., Lu, J., Zheng, H., et al. (2020). Investigation on expansion effect of the expansive agents in ultra-high performance concrete. *Cem. Concr. Compos.* 105, 103425. doi:10.1016/j.cemconcomp.2019.103425
- Wang, T., Gong, J., Chen, B., Gong, X., Luo, H., Zhang, Y., et al. (2021). Effects of shrinkage reducing agent and expanded cement on UHPC fluidity, mechanical properties, and shrinkage performance. *Adv. Mater. Sci. Eng.* 2021, 1–14. doi:10.1155/2021/9045754
- Wang, Y., Tian, Q., and Li, H. (2022). Humidity sensitivity of hydration of expansive agent and its expansive efficiency in ultra-high performance concrete. *Crystals* 12 (2), 195. doi:10.3390/cryst12020195
- Xu, Y. M. (2014). Quantitative determination of periclase and periclase hydration in high magnesium cement clinker with XRD internal standard method. *J. Nanjing Tech Univ.* 36 (5), 30–35. (in Chinese). doi:10.3969/j.issn.1671-7627.2014.05.006
- Yang, J., Li, S., and Feng, Y. (2021). Expansion mechanism and properties of magnesium oxide expansive hydraulic cement for engineering applications. *Adv. Mater. Sci. Eng.* 1–9. doi:10.1155/2021/5542072
- Yoo, D. Y., Park, J. J., Kim, S. W., and Yoon, Y. S. (2013). Early age setting, shrinkage and tensile characteristics of ultra high performance fiber reinforced concrete. *Constr. Build. Mat.* 41, 427–438. doi:10.1016/j.conbuildmat.2012.12.015
- Yoo, D. Y., Kim, S., Lee, J. Y., You, I., and Lee, S. J. (2019). Implication of calcium sulfoaluminate-based expansive agent on tensile behavior of ultra-high-performance fiber-reinforced concrete. *Constr. Build. Mater.* 217, 679–693. doi:10.1016/j.conbuildmat.2019.05.071